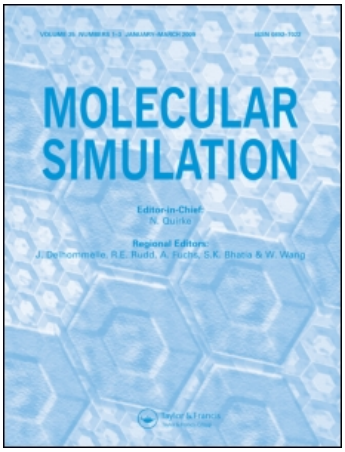

Molecular Simulation
Publication details, including instructions for authors and subscription information:
http://www.informaworld.com/smpp/title~content=t713644482

The Rheology of *n*-Butane and *i*-Butane by Non-Equilibrium Molecular Dynamics Simulations

Song Hi Lee[a]; Peter T. Cummings[b]
[a] Department of Chemistry, Kyungsung University, Pusan, Korea [b] Department of Chemical Engineering, University of Tennessee, Knoxville, TN, U.S.A.

To cite this Article Lee, Song Hi and Cummings, Peter T.(1996) 'The Rheology of *n*-Butane and *i*-Butane by Non-Equilibrium Molecular Dynamics Simulations', Molecular Simulation, 16: 4, 229 — 247
To link to this Article: DOI: 10.1080/08927029608024077
URL: http://dx.doi.org/10.1080/08927029608024077

Molecular Simulation, 1996, Vol. 16, pp. 229–247
Reprints available directly from the publisher
Photocopying permitted by license only

THE RHEOLOGY OF *n*-BUTANE AND *i*-BUTANE BY NON-EQUILIBRIUM MOLECULAR DYNAMICS SIMULATIONS

SONG HI LEE

Department of Chemistry, Kyungsung University, Pusan, Korea 608-736

PETER T. CUMMINGS

Department of Chemical Engineering, University of Tennessee, Knoxville, TN 37996-2200, U.S.A.

(Received December 1994, accepted July 1995)

We present non-equilibrium molecular dynamics (NEMD) simulations of planar Couette flow for models for normal (*n*-butane) and isomeric butane (*i*-butane) molecules. Two of the three classes of models used here are collapsed atom models while the third class is an atomistically detailed model. In general agreement with previous workers, we find that the collapsed atom models predict the viscosity of the *n*-butane quite well. However, if the collapsed atom models are applied to the isomer by simply changing the geometry of the molecule, one finds that the viscosity is underpredicted. The atomistically detailed model considered here is an amalgam of several models. We find that our atomistically detailed model does not yield quantitative agreement with the viscosity of either the *n*-butane or its isomer. However, the atomistically detailed model does have the one positive feature that if it is applied to the isomer by simply changing the geometry of the molecule, one finds that the viscosity increases in agreement with experiment. This suggests that atomistically detailed models may hold the key to developing a set of group-group interactions which can be used equally well to predict the viscosity of normal and isomeric alkane fluids.

KEY WORDS: Non-equilibrium molecular-dynamics, *n*-butane, *i*-butane, rheology, atomistically detailed models.

1 INTRODUCTION

Non-equilibrium molecular dynamics (NEMD) simulation is a powerful and efficient method for studying bulk and microscopic fluid properties for system subject to homogeneous shear. The transport properties of many systems have been predicted by NEMD and its applications are reviewed by Cummings and Evans [1]. Evans and his coworkers have used NEMD to study the rheological behavior of liquid alkanes such as butane, decane, eicosane, tridecane, and 5-butyl nonane under homogeneous shear in NVT and NpT ensembles [2–5]. Initially, the alkane model used by them was the Ryckaert-Bellemans (RB) collapsed atom model [6–9] in which methyl and methylene groups are represented by spheres interacting via Lennard-Jones (LJ) potentials. The main benefit of this model is to reduce a considerable amount of computing time by reducing the number of interaction sites. In

their later work [3–5], they replaced the LJ potentials by LJ potentials truncated at its minimum $r = 2^{1/6}\sigma$, and shifted so that the potential is zero at the point of truncation. This potential is often referred to as the Weeks-Chandler-Andersen (WCA) prescription [10–11].

Chynoweth and his coworkers have adopted and expanded the RB model by accounting for intramolecular interactions between the RB blobs [12]. For this, bond stretching and bond angle bending potentials have been added to the original torsional potential of the RB model. They used this model for the rheological properties of liquid *n*-butane [13] and liquid *n*-hexadecane [14] by NEMD simulation method. They reported a behavior [13] of strain-rate dependent viscosity of *n*-butane, *i.e.*, the linear dependence of viscosity on $\gamma^{1/2}$, which is different from Evans and his coworkers' result, *i.e.*, an intermediate Newtonian region around 10^{11} s^{-1} and a second shear-thinning region at higher shear rates [2]. They also reported a NEMD study of liquid *n*-hexadecane [14]. In their study, although low-shear-rate simulations are restricted by long computational times, for the given model the onset of the non-Newtonian region is estimated to be around 10^{10} s^{-1} and the liquid's first Newtonian regime is clearly seen.

In this paper, we examine the Newtonian and strain-rate dependent rheological properties of several models for *n*-butane and *i*-butane. Our models are three different ones, *i.e.*, the original RB collapsed atom model [6–9], the expanded second collapsed atom model [12–14] and finally an atomistically detailed model. Particularly in the third model, there is a possibility that the dynamics associated with the rheological properties may be quite different. For example, in the study of penetrant diffusion-the diffusion of low molecular weight species in a polymer melt–Muller-Plathe *et al.* [15–18] showed that models for polymer melts analogous to the RB collapsed atom model and the atomistically detailed model differ by two orders of magnitude in the predicted penetrant diffusion rates. They also pointed out that only the atomistically detailed model agreed well with experimental data. The reason for the difference in penetrant diffusion rates was the better representation of the fluctuation of the energy surface with polymer motion in the atomistically detailed model so that the energy activated jumps between cavities which are the rate limiting part of penetrant diffusion are more faithfully reproduced in the atomistically detailed model. Since viscosity can be thought of, and is frequently modeled, as an energy activated process, it is reasonable to assume that atomistically detailed models may give rise to significantly different dynamics. The use of atomistically detailed models to describe polymer melts is reviewed by Gusev *et al.* [19].

2 LIQUID ALKANE MODELS AND MOLECULAR DYNAMICS SIMULATION

Models with varying degrees of detail are used for studying transport phenomena in polymeric fluids. The coarsest model is the bead and spring model in which twenty or more monomeric units of the polymer chain are lumped together as a single spherical unit (bead) and the net intramolecular interaction between beads is modeled by a spring interaction [20]. There are several variations on this basic model,

including the case of finitely extensible non-linear elastic (FENE) interactions between beads [21–24]. Bead and spring models are expected to yield an accurate picture for the steady state rheological properties of real polymer solution in the dilute regime [20]. The restriction to steady state is that bead and spring models ignore many of short time scale motions of the polymer and focus instead on the long time dynamics represented by the springs.

At the next level of detail are the so-called collapsed atom models, in which monomeric units (methylene or methyl) are typically treated as a single sphere with a LJ potential between the spheres. In Ryckaert and Bellemans' original collapsed atom model [6–9], a C—C—C—C torsional rotation potential is also included: The methyl and methylene groups in alkanes are treated as spheres with mass of 2.411×10^{-26} kg. The distance between neighboring spheres is fixed at 0.153 nm and the bond angles are fixed at 109.47°. The torsional potential acts between each pair of spheres that are three apart on the alkane chain. Not only sites on different molecules but spheres more than three apart on the same molecule interact through as 12–6 LJ potential with parameters $\sigma = 0.3923$ nm and $\varepsilon/k_B = 72$ K. We shall refer to this model as model I in this work.

The second collapsed atom model we consider is that of Chynoweth *et al.* [12–14] which includes C—C bond stretching and C—C—C bond angle bending potentials [25]

$$V(r_{ij}) = \mathrm{K}_0 (r_{ij} - r_e)^2 \tag{1}$$

$$V(\theta) = \mathrm{K}_1 (\theta - \theta_e)^2 - \mathrm{K}_2 (\theta - \theta_e)^3 \tag{2}$$

where $r_e = 0.153$ nm, $\theta_e = 109.47°$, and the force constants K_0, K_1, and K_2 are given by 132552 kJ/mol·nm^2, 0.0502092 kJ/mol·deg^2, and 0.000482 kJ/mol·deg^3, respectively. The other potentials, torsional and LJ, are the same as model I. We shall refer to this model as model II. More refined collapsed atom alkane models are described by Toxvaerd [26].

The third model we consider is the so-called atomistically detailed model in which all the atoms in the monomeric units are represented explicitly in the model for the molecules [15–18, 27]. That is, carbon (C) and hydrogen (H) atoms are treated explicitly. Between non-bonded particles, there are LJ 12–6 potentials ($u_{\mathrm{CC}}(r)$, $u_{\mathrm{CH}}(r)$, and $u_{\mathrm{HH}}(r)$ with the Lorentz-Berthelot mixing rules used to obtain the cross interaction), C—C and C—H stretching potentials, C—C—C, C—C—H, and H—C—H bond angle bending potentials, and C—C—C—C and the ending C—C—C—H torsional rotational potentials. The bond stretching potential is the same form of Eq. 1 but the bond angle bending potential has the form of Eq. 1 rather than Eq. 2. The ending C—C—C—H torsional potential has a different form from the C—C—C—C one:

$$V(\alpha) = \mathrm{K}_3 (1 - 4\cos^3\alpha + 3\cos\alpha) \tag{3}$$

Initially, we used the potential parameters developed by Muller-Plathe *et al.* [27] for polyisobutylene except the C—C—C—C torsional parameters for the original Ryckaert and Bellemans' model [6–9] were used. The NEMD results for *n*-butane and *i*-butane with these potential parameters were at strong variance with experiment. At a density of 0.583 g/cc and temperature of 291 K, the calculated

pressure was approximately -1000 atm in the absence of shear (when one should expect a value of 1 atm) and, when the system was subjected to homogeneous shear so that the x-component of the streaming velocity varied in the y-direction, the calculated density profiles showed a density inhomogeneity in the y-direction as in Figure 1. In switching to an NpT ensemble simulation at pressure of 1 atm and temperature of 291 K, the density in the absence of shear was found to be 0.722 g/cc, much higher than the expected value of 0.583 g/cc. We concluded that these potentials – in particular, the LJ parameters – are not appropriate for describing short alkane chains.

Potential parameters for the atomistically detailed models of alkanes are rarely reported in the literature. In the MD study of n-alkane tricosane by Ryckaert *et al.* [28] they used a flexible-chain model in which the hydrogen atoms are incorporated explicitly, and the C—C and C—H bond lengths, and the H—H distances in CH_2 and CH_3 are constrained as constants. The intermolecular potential between atoms consists of "exp-6" interactions. We inferred LJ parameters from the exp-6 parameters by keeping the position of the potential minimum unchanged. The resulting LJ potentials are in good agreement with the original exp-6 potentials. For example, the C—C potential curves of both exp-6 and LJ potentials are compared in Figure 2. The set of LJ parameters obtained in this way do not follow the Lorentz-Berthelot mixing rule and the σ for H atom seems slightly large. The LJ parameters for H atom are modified to comply with the mixing rule. The final values of potential parameters for the third model, which we subsequently refer to as model III, are given in Table 1. The results of NEMD for n-butane and i-butane give almost the same LJ energy as the models I and II but the calculated pressures are very high (about 1000 atm), similar to that of model I.

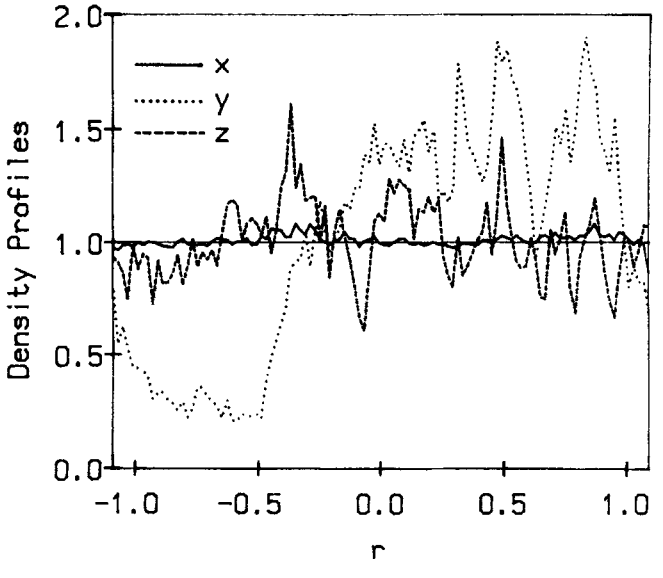

Figure 1 Normalized density profiles of model III for n-butane at $T = 291$ K and $\rho = 0.583$ g/cc with $\gamma = 1.0$ ps^{-1} using Muller-Plathe *et al.* potential [27].

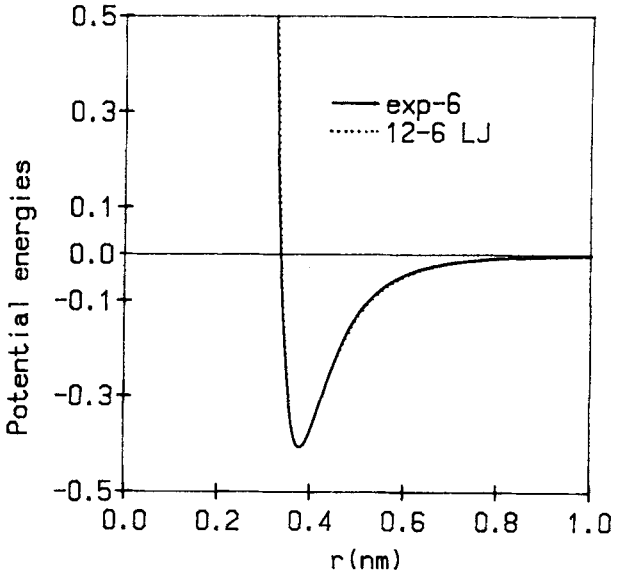

Figure 2 Comparison of potential curves of C—C "exp-6" and C—C LJ interactions.

Table 1 Potential parameters for the atomistically detailed model, model III.

LJ parameters	σ(nm)*	ε(kJ/mol)*
C—C	0.33665 (0.3207)	0.40561 (0.3519)
C—H	0.30561 (0.2763)	0.17219 (0.3345)
H—H	0.27457 (0.2318)	0.07310 (0.3180)
bond Stretching	r_e(nm)	K_0(k J/mol·nm^2)
C—C	0.153	210000
C—H	0.110	147000
bond angle bending	θ_e(deg)	K_1(kJ/mol·deg^2)
C—C—C	111.0	0.0734584
C—C—H	109.5	0.0558821
H—C—H	107.9	0.0466674
torsional	K_3(kJ/mol)	
C—C—C—C	Ryckaert-Bellemanns'	(Refs. 6–9)
C—C—C—H	11.72	

*( ) are Muller-Plathe *et al*'s.

For the study of planar Couette flow, in which fluids are subjected to homogeneous shear between two parallel plates located at infinity, the NEMD algorithm for alkane is a molecular version of the SLLOD algorithm [29]. The equations of motion for site s in molecule i are given by

$$d\mathbf{r}_{is}/dt = \mathbf{p}_{is}/m_s + \mathbf{n}_x\gamma y_i \tag{4}$$

$$d\mathbf{p}_{is}/dt = \mathbf{F}_{is} - \mathbf{n}_x(m_s/M)\gamma p_{yi} - \alpha(m_s/M)\mathbf{p}_i \tag{5}$$

where $M = \Sigma_s m_s$, $\mathbf{r}_i = \Sigma_s (m_s/M)\mathbf{r}_{is}$, $\mathbf{p}_i = \Sigma_s \mathbf{p}_{is}$, and $\mathbf{F}_i = \Sigma_s \mathbf{F}_{is}$. $\mathbf{n}_x$ is the unit vector in the x-direction, $\mathbf{F}_{is}$ is the force exerted by the other sites in the same and different molecules on the site s in molecule i, γ is the strain rate, $\partial u_x/\partial y$, and α, is the thermostatting constant, given by

$$\alpha = \frac{\sum_{i=1}^{N} [\mathbf{F}_i \cdot \mathbf{p}_i - \gamma p_{yi} p_{xi}]}{\sum_{i=1}^{N} p_i^2} \tag{6}$$

The effect of the thermostatting term involving $\alpha(m_s/M)\mathbf{p}_i$ in Eq. 5 is to hold the translational center-of-mass kinetic energy constant. The momenta in Eqs. 4 and 5 are measured with respect to the streaming velocity of the fluid and are known as peculiar momenta.

The pressure tensor $\mathbf{P}$ is expressed in terms of molecular quantities by

$$\mathbf{P}V = \sum_{i=1}^{N} \mathbf{p}_i \mathbf{p}_i / M + \sum\sum_{1 \leqslant i \leqslant j < N} \mathbf{r}_{ij} \mathbf{F}_{ij} \tag{7}$$

where V is the volume of the system, $\mathbf{r}_{ij} = \mathbf{r}_i - \mathbf{r}_j$ is the vector joining the centers of molecules i and j, and $\mathbf{F}_{ij}$ is the force between them. These equations of motion are combined with the Lees-Edwards "sliding brick" boundary conditions [30]. In the absence of the thermostat, the terms in Eqs. 4 and 5 involving the strain field, γ, cancel to yield Newton's equations of motion relating $\mathbf{r}_i$ and $\mathbf{F}_i$. This implies that the SLLOD algorithm truly generates boundary driven planar Couette flow, leading to the conclusion that it is correct to arbitrary order in the strain rate when appropriately thermostatted [27]. The strain rate dependent shear viscosity is then obtained from Newton's law of viscosity

$$\eta = -(P_{xy} + P_{yx})/2\gamma \tag{8}$$

where P_{xy} and P_{yx} are the averaged xy and yx components of $\mathbf{P}$. From kinetic and mode coupling theories, it is known that the strain rate dependence of the shear viscosity is linear in $\gamma^{1/2}$ [31–33]. Hence, to apply the SLLOD algorithm to a Newtonian fluid, one performs several simulations at different strain rates γ and fits the resulting strain rate dependent viscosities to the equation

$$\eta = \eta_0 + \eta_1 \gamma^{1/2} \tag{9}$$

The zero strain rate extrapolation of η, η_0, is thus the Newtonian viscosity.

A canonical ensemble of fixed N (= 64 butane molecules), V (length of cubic box, $L = 2.198$ nm), and T ($T = 291$ K) is chosen for the simulation ensemble. Gauss's principle of least constraint [34] is used to maintain the system at a constant temperature according to Eqs. 5 and 6. The ordinary periodic boundary condition in the x-, y-, and z-directions and minimum image convention for the LJ potential are applied with a spherical cut-off distance of radius 0.9808 nm for models I and II, and 0.8416 nm for model III. The NEMD simulation for model I is performed using the Verlet algorithm for the integration of the equations of motion [35] with a time step of 2 fs and the RATTLE algorithm [36] is used to impose the bond length and angle constraints. The ones for models II and III are performed using Gear's fifth order predictor-corrector method [37] with time steps of 1 fs for model II and 1/3 fs for

model III. For each system, 9 strain rates are simulated. Each strain rate requires approximately 50,000 time steps for the attainment of steady state, and for sampling the rheological properties different time steps are needed according to the strain rates – 300,000 time steps for $\gamma = 0.04$ ps^{-1}, 240,000 for 0.09 and 0.16, 160,000 for 0.25, 0.36, and 0.49, 100,000 for 0.64, 0.81, 1.0, and 0.0. The equilibrium properties of liquid *n*-butane and *i*-butane are summarized in Table 2.

3 RESULTS

We begin by comparing the strain rate dependent viscosities of models I and II for *n*-butane at density 0.583 g/cc and temperature 291 K with those of Edberg *et al.* [2] and Chynoweth *et al.* [13]. Our results will be given in terms of the real strain rates, while a dimensionless strain rate is defined by $\gamma^* = \delta\sigma(m/\varepsilon)^{1/2}$. Thus, for *n*-butane and *i*-butane, $\gamma^* = 1$ corresponds $\gamma = 5.2 \times 10^{11}$ see^{-1}. As shown in Figure 3, when Edberg *et al.*, plotted their calculated viscosities of model I for *n*-butane against $\gamma^{1/2}$, they inferred an intermediate Newtonian region around 10^{11} sec^{-1} and a second shear-thinning region at higher shear rates. The same kind of effect was observed in the NEMD simulations of *n*-butane and *i*-butane by Rowley and Ely [38], in which η^* $[\eta\sigma^2/(m\varepsilon)^{1/2}]$ of both liquids $[T^*$ $(k_BT/\varepsilon) = 1.871$ and ρ^* $(\rho\sigma^3) = 1.85]$ appear quite linear with $\gamma^{*1/2}$ over the ranges $0 < \gamma^* < 0.16$ and $\gamma^* > 1.0$ with different slopes, but they appear to be nearly independent of $\gamma^{*1/2}$ in the range $0.25 < \gamma^* < 1.0$. The code used in their work was modified from that used by

Table 2 Equilibrium properties of model III for liquid *n*-butane and *i*-butane.

properties	*n-butane*	*i-butane*
molecular temperature (K)	291.0 ± 0.4	291.0 ± 0.0
atomic temperature (K)	287.5 ± 47.3	335.8 ± 5.9
pressure (atm)	1142 ± 379	1131 ± 69
total LJ energy	−16.86 ± 0.68	−15.43 ± 0.58
inter C—C LJ energy (kJ/mol)	−6.807 ± 0.047	−6.509 ± 0.026
inter C—H LJ energy	−10.03 ± 0.11	−9.706 ± 0.025
inter H—H LJ energy	−0.804 ± 0.296	−0.843 ± 0.50
intra C—H LJ energy	−0.359 ± 0.050	–
intra H—H LJ energy	1.140 ± 0.181	1.632 ± 0.030
C—C—C—C torsional energy	2.571 ± 0.404	–
C—C—C—H torsional energy	1.874 ± 0.344	3.867 ± 0.087
C—C stretching energy	3.618 ± 0.805	4.171 ± 0.157
C—H stretching energy	12.99 ± 2.64	16.01 ± 0.26
C—C—C angle bending energy	2.103 ± 0.339	2.870 ± 0.115
C—C—H angle bending energy	13.63 ± 2.78	13.72 ± 0.43
H—C—H angle bending energy	7.962 ± 1.532	10.32 ± 0.24
average C—C bond length (nm)	0.1531 ± 0.0001	0.1532 ± 0.0000
average C—H bond length	0.1100 ± 0.0002	0.1100 ± 0.0000
average C—C—C bond angle (°)	111.79 ± 0.37	110.72 ± 0.03
average C—C—H bond angle	109.63 ± 0.21	109.76 ± 0.00
average H—C—H bond angle	108.35 ± 0.18	108.41 ± 0.03
average % of C—C—C—C trans	86.9 ± 3.5	–
rms end-to-end length (nm)	0.3795 ± 0.0025	0.2522 ± 0.0001
rms radius of gyration	0.1465 ± 0.0009	0.1278 ± 0.0001

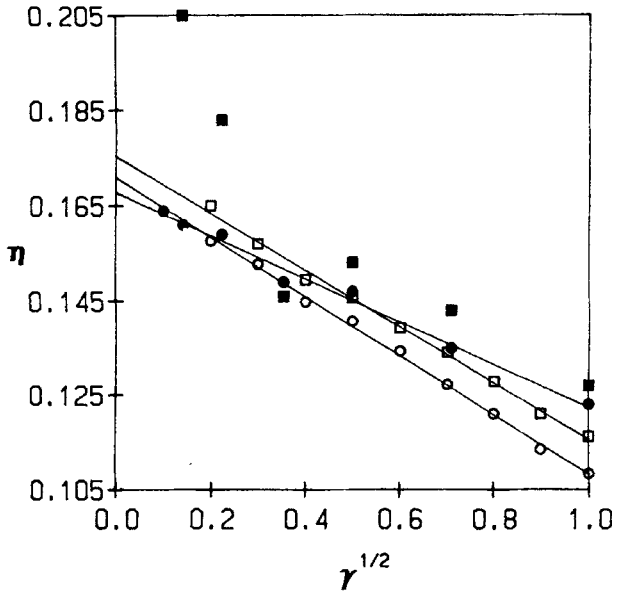

Figure 3 Strain rate dependent viscosities of models I and II of *n*-butane. Filled squares: Edberg *et al.* [2] results for model I, open squares: our results for model I, filled circles: Chynoweth *et al.* [13] results for model II, and open circles: our results for model II.

Edberg *et al.* [2] However, the result of model II for *n*-butane by Chynoweth *et al.* [13] showed that these effects disappear and the linear dependence of viscosity on $\gamma^{1/2}$ at low shear rates has been maintained. Our results for both models for *n*-butane followed the Chynoweth *et al*'s trend. Edberg *et al.* [2] obtained 0.24 cP from their NEMD simulations and Marechal and Ryckaert [39] arrived at 0.26 cP from EMD via the Green- Kubo relation. Chynoweth *et al.* [13] obtained 0.168 cP by a linear extrapolation of their calculated viscosities. Our results given 0.175 cP for model I and 0.171 cP for model II which are closer to the experimental value on (0.19 cP[40]). This agreement with the experimental result might be fortuitous because all the models used are the collapsed atom models. There is a slight difference between our results and Chynoweth *et al*'s result, even though the interaction potentials are the same.

The strain rate dependent viscosities of models I and II for *n*-butane and *i*-butane are compared in Figure 4. The dependence of the calculated viscosities models I and II of *i*-butane on $\gamma^{1/2}$ appear almost linear as do those of *n*-butane. Both models for *n*-butane and *i*-butane liquids are shear-thinning, although both models of *n*-butane are slightly more shear-shinning than those of *i*-butane. The Newtonian viscosities for *i*-butane obtained by a linear extrapolation to $\gamma = 0$ are 0.158 cP for model I and 0.153 cP for model II, respectively. Thus, the viscosity of *i*-butane is predicted by both models I and II to be less than that of *n*-butane. This trend agrees with the general results of Rowley and Ely [38], who also found that accounting for structural differences alone in the intermolecular potentials does not account for the observed differences in viscosities of the two fluids. Although branching does affect

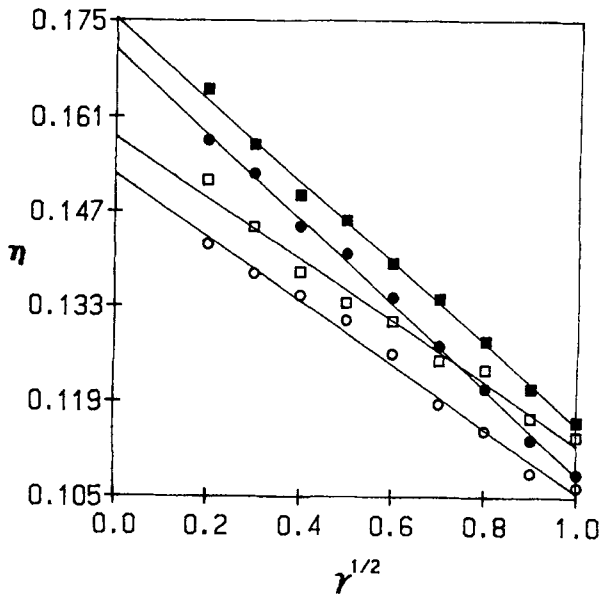

Figure 4 Strain rate dependent viscosities of models I and II of *n*-butane and *i*-butane. Filled squares: model I for *n*-butane, open squares: model II for *n*-butane, filled circles: model I for *i*-butane, and open circles: model II for *i*-butane.

the viscosity, the NEMD predicts a lowering of the viscosity relative to its straight-chain counterpart at equivalent reduced conditions, in apparent contradiction to the experimentally observed behaviour (in which viscosity is found to increase with branching). Other factors must outweigh the decrease in reduced viscosity due to branching. Rowley and Ely's solution [38] was to use larger LJ size parameters for *i*-butane than for *n*-butane. After doing so, they were able to obtain good agreement with experiment over a large range of density.

The branching effect in models I and II for *n*-decane and 4-propyl heptane will be discussed in a future paper [41]. Our NEMD results of the shear-induced viscosities using models I and II showed that branching lowers the viscosity as observed in the case of *n*-butane and *i*-butane. But in the NEMD simulations of model I for 5-butyl nonane and *n*-tridecane with WCA-type [10–11] potential by Daivis and Evans [4], the branched alkane exhibits higher viscosity than the straight chain molecule, which is the opposite of what was found for butane.

We now turn our attention to the model III of *n*-butane and *i*-butane. The strain rate dependent viscosities are shown in Figure. 5. Although the value of the viscosities is too high compared to experiment, we see that the NEMD simulations show that branching increases viscosity. This result is exactly opposite to those of models I and II of *n*-butane and *i*-butane and agrees with the experimental trend. This suggests that the inclusion of H atoms (and accordingly the consideration of H—H and C—H LJ, and C—H and H—H bond stretching, and C—C—H and H—C—H angle bending interactions) in intermolecular and intramolecular

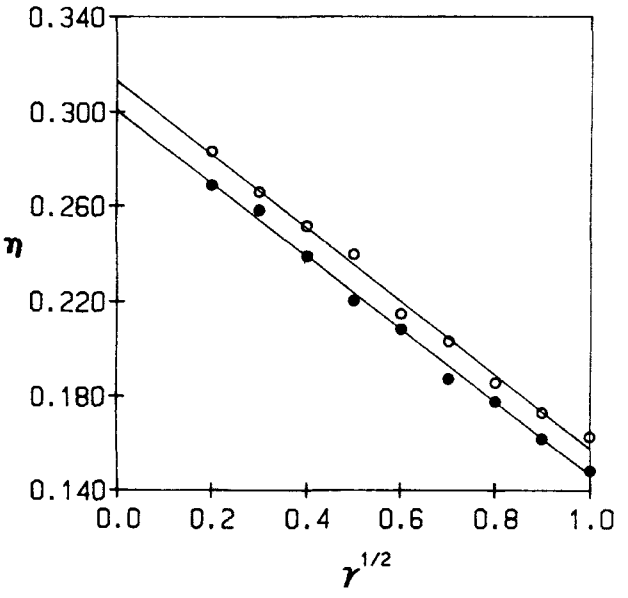

Figure 5 Strain rate dependent viscosities of model III of *n*-butane and *i*-butane. Filled circles: *n*-butane and open circles: *i*-butane.

potential models may be important in correctly predicting the effect of molecular structure on alkane rheology.

The material functions are related by the normal stress differences by $\Psi_1 r^2 = P_{yy} - P_{xx}$ and $\Psi_2 r^2 = P_{zz} - P_{yy}$ [19] Figures 6 and 7 show the normal stress differences of model III for *n*-butane and *i*-butane as function of $\gamma^{3/2}$. The signs of Ψ_1 and Ψ_2 are in agreement with typical experimental results for non-Newtonian fluids, $\Psi_1 > 0$ and $\Psi_2 < 0$. The ratio $-\Psi_2/\Psi_1$ increases with increasing shear rate from 0.5 to 1.0 for *n*-butane and from 0.4 to 3.0 for *i*-butane. Experimental measurements on non-Newtonian fluids typically results in values of < 0.4 and simple fluid NEMD studies give the result $-\Psi_2/\Psi_1 \approx 1$ [42]. In Figure 8, we show the scalar pressure difference, $p(\gamma) - p(0)$, as function of $\gamma^{3/2}$. The equilibrium pressures of model III for *n*-butane and *i*-butane are extremely high, about 1140 and 1130 atm. Those of model I for *n*-butane and *i*-butane are about 1050 and 1000 atm, and for model II, about 400 and 350 atm, respectively. The pressure difference of both fluids is nearly linear vs $\gamma^{3/2}$ over all the range of γ and *i*-butane pressure increases more rapidly with increasing shear rate than n-butane pressure does.

The birefringence parameter, the shear-induced molecular alignment, can be monitored by the symmetric order tensor, $\mathbf{S} = (1/N) \sum_i \mathbf{R}_i \mathbf{R}_i$, where the arbitrary orientation vector $\mathbf{R}_i$ is taken to be the end-to-end C—C vector for *n*-butane molecules and the average vector of three end-to-end C—C vectors for *i*-butane molecules. The normalized birefringence (order tensor) is obtained by $\mathbf{S}_o = \mathbf{S}/Tr(\mathbf{S})$. In an orientationally isotropic fluid $\mathbf{S}_o = 1/3\ \mathbf{U}$ where $\mathbf{U}$ is the unit tensor. Figures 9 and 10 show the diagonal and the *xy* component of the normalized order tensors of model III for *n*-butane and *i*-butane, respectively, indicating that *n*-butane

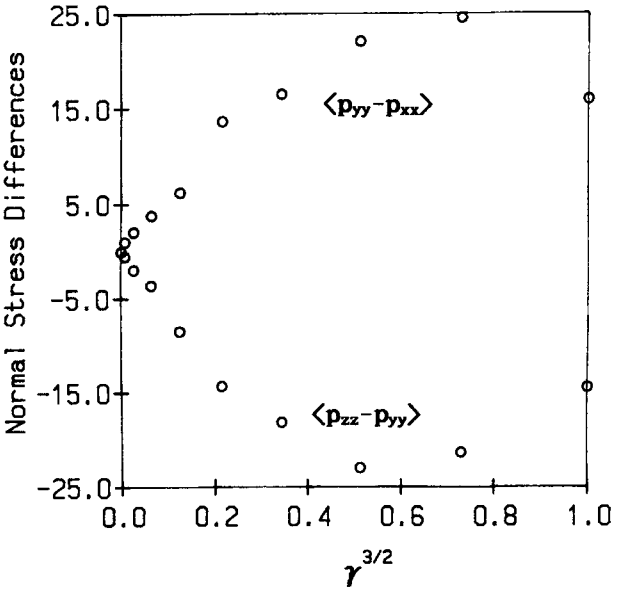

Figure 6 Normal stress differences of model III for *n*-butane.

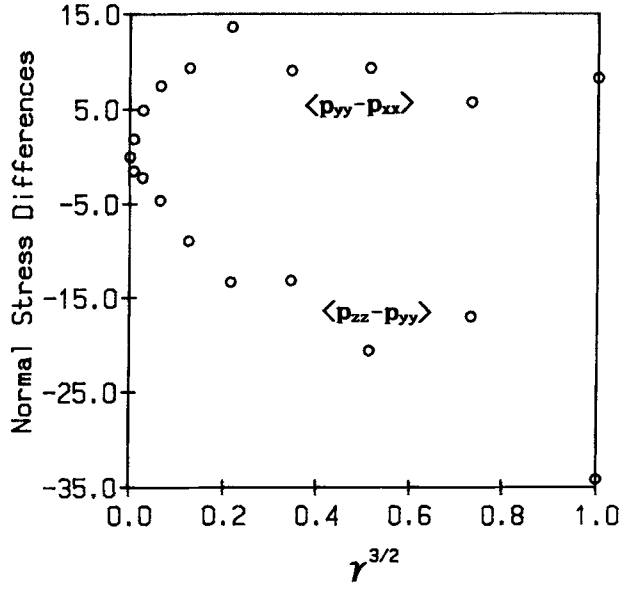

Figure 7 Normal stress differences of model III for *i*-butane.

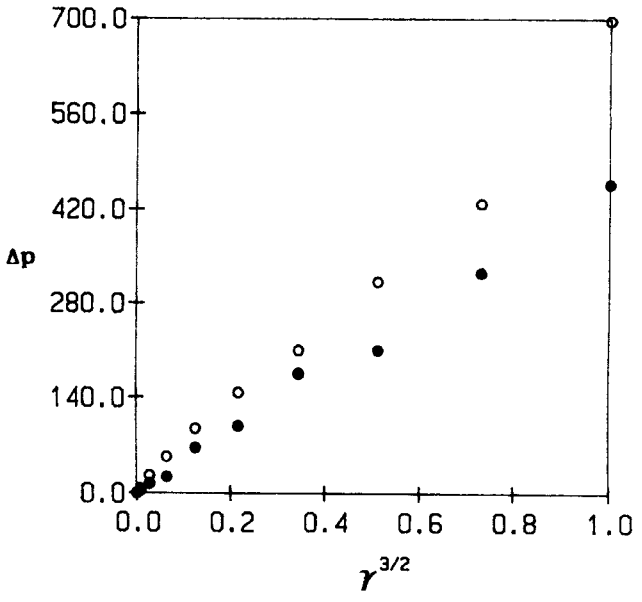

Figure 8 Shear dilation, $p(\gamma)-p(0)$. Filled circles: model III for *n*-butane and open circles: model III for *i*-butane.

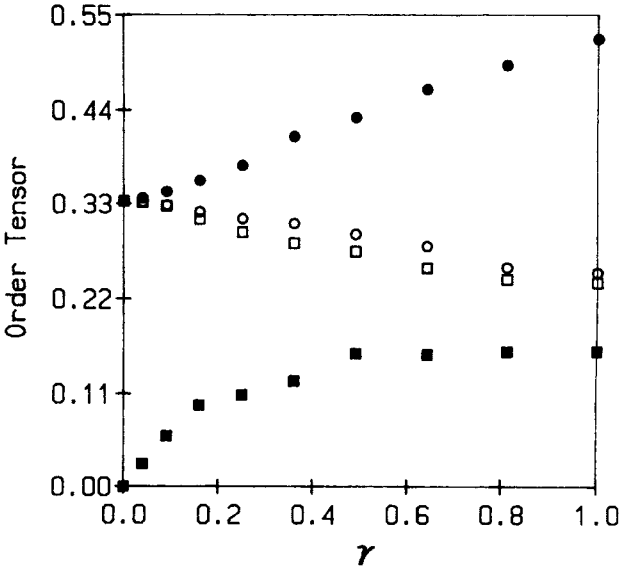

Figure 9 Normalized order tensor of model III for *n*-butane. Filled circles: S^{o}_{xx}, open circles: S^{o}_{zz}, open squar: S^{o}_{yy} and filled squares: S^{o}_{xy}.

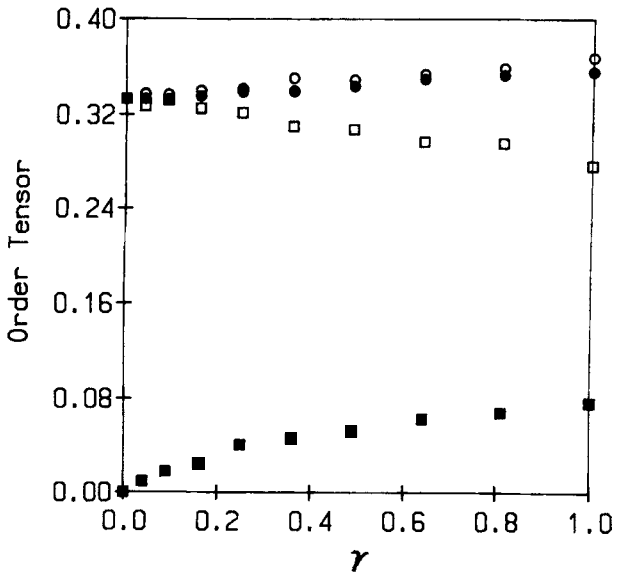

Figure 10 Normalized order tensor of model III for *i*-butane. Filled circles. S^o_{xx}, open circles: S^o_{zz}, open squares: S^o_{yy}, , and filled squares: S^o_{xy}.

molecules are substantially aligned along the shear field while *i*-butane molecules are less clearly aligned due to its higher symmetry.

In Figures 11 and 12, we show the mean squared end-to-end C—C distance and radius of gyration about center of mass of model III for *n*-butane and *i*-butane, and the average trans population of model III for n-butane as function of γ. For the case of *n*-butane, these properties increase with increasing shear rate as expected. The elongation of *n*-butane upon shearing is consistent with the increase of trans population, even there are other factors for molecular deformation, bond stretching and angle bending. However, the mean squared end-to-end distances and radius of gyration of *i*-butane decrease with increasing shear rate, although the change is very small. Since there is no C—C—C—C torsional interaction in *i*-butane, this change comes from the bond stretching and angle bending.

The total Lennard-Jones and torsional energies per molecule of model III for *n*-butane and *i*-butane are shown in Figures 13 and 14. Both torsional energies (C—C—C—C and C—C—C—H) decrease with increasing shear rate, consistent with the average trans population, but later begins to saturate. The total LJ energy of *n*-butane is lower than that of *i*-butane by about 1.0 kJ/mol, but the sum of these energies is almost the same at high shear rates. In Figures 15 and 16, we show the inter C—C, C—H and H—H, and intra C—H and H—H LJ energies per molecule of model III for *n*-butane and *i*-butane. All the LJ energies decrease very slowly with increasing shear rate except the increasing inter H—H LJ energies. The inter C—C and C—H LJ energies of *n*-butane are lower than those of *i*-butane by about 0.5 kJ/mol respectively. The intra H—H repulsion is much bigger

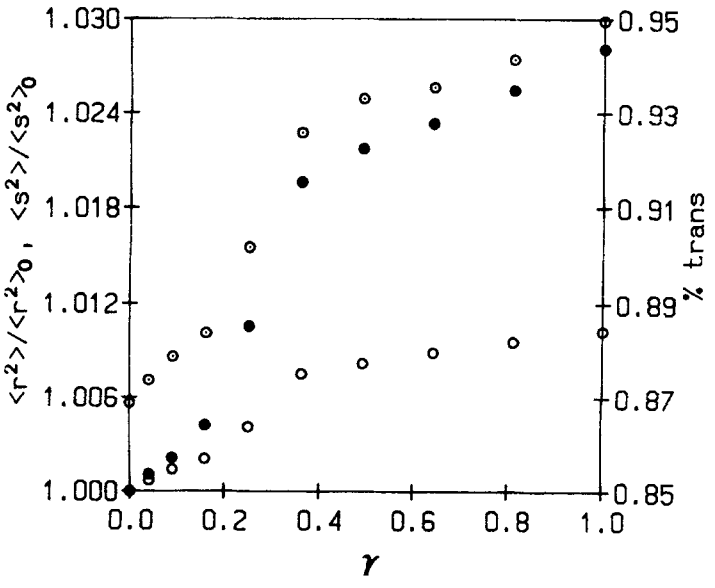

Figure 11 % C—C—C—C trans(⊙), mean squared end-to-end distance (●), and radius of gyration squares (●) of model III for *n*-butane.

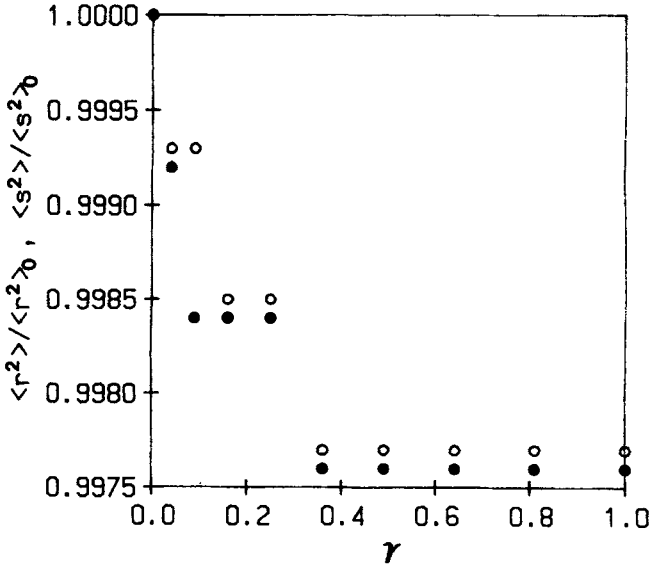

Figure 12 Mean squared end-to-end distance (●) and radius of gyration (○) of model III for *i*-butane.

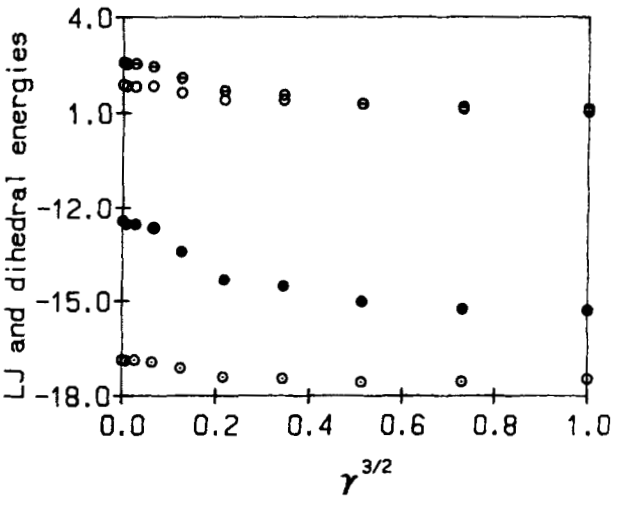

Figure 13 C—C—C—C torsional energy (⊖), C—C—C—H torsional energy (○), total LJ energy (⊙) and the sum of these three energies (●) of model III for *n*-butane.

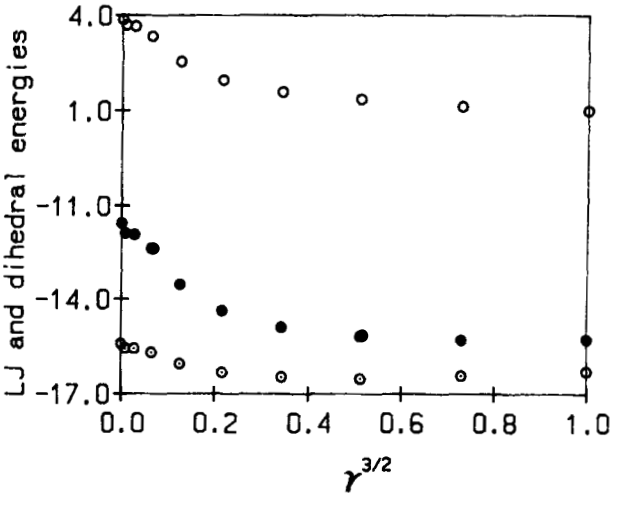

Figure 14 C—C—C—H torsional energy (○), total LJ energy (⊙), and the sum of these two energies (●) of model III for *i*-butane.

than that of *n*-butane at low shear rates but becomes almost equal at high shear rates. Finally the C—C and C—H bond stretching and C—C—C, C—C—H and H—C—H bond angle bending energies of model III for *n*-butane and *i*-butane per molecule per mode are shown in Figures 17 and 18. The C—C bond stretching

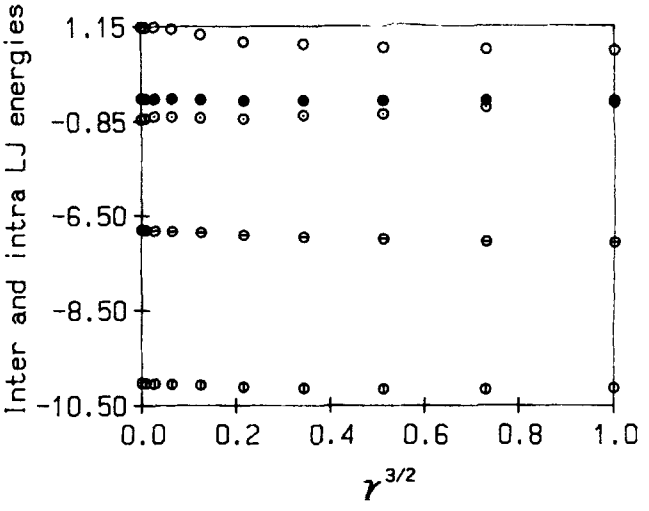

Figure 15 Intra C—H LJ aenergy (●), intra H—H LJ energy (○), inter C—C LJ energy (⊖), inter C—H LJ enegy (◫), and inter H—H LJ energy (⊙) of model III for *n*- butane.

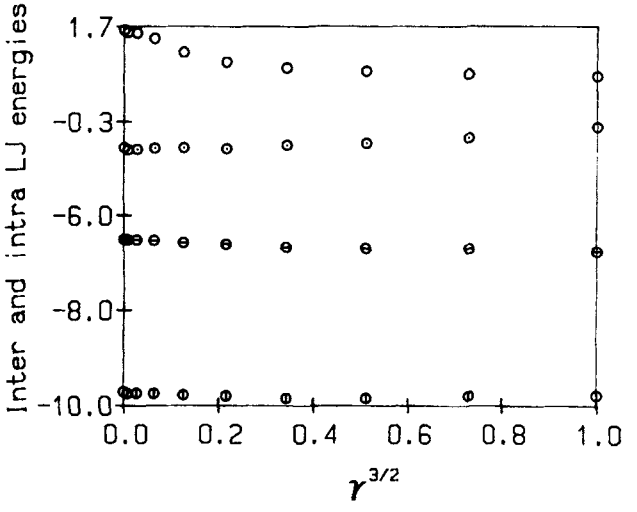

Figure 16 Intra H—H LJ energy (○), inter C—C LJ energy (⊖), inter C—H LJ energy (◫), and inter H—H LJ energy (⊙) of model III for *i*-butane.

and C—C—C bond angle bending energies of both fluids decrease smoothly with increasing shear rate as expected because of the absence of H atom in vibrational motions. The other H atom-included vibrational energies drop very rapidly at shear rate of 0.125 ps^{-1} and these vibrations are almost frozen at their fixed bond length and bond angles similar to that of rigid molecule.

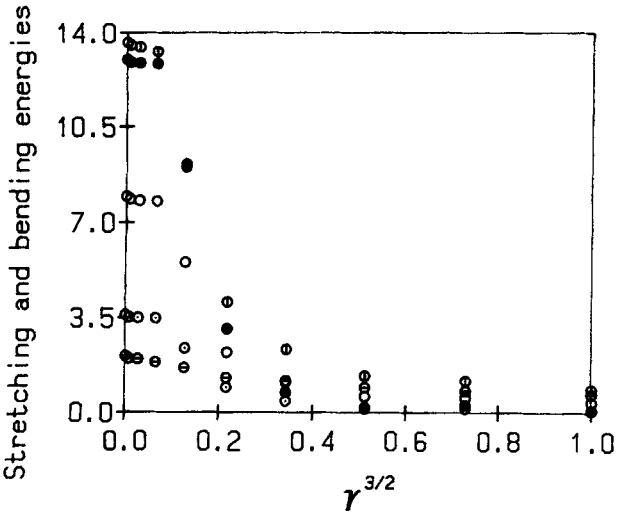

Figure 17 C—C bond stretching energy (⊙), C—H bond stretching energy (●), C—C—C bond angle bending energy (⊖), C—C—H bond angle bending energy (◫), and H—C—H bond angle bending energy (○) of model III for *n*-butane.

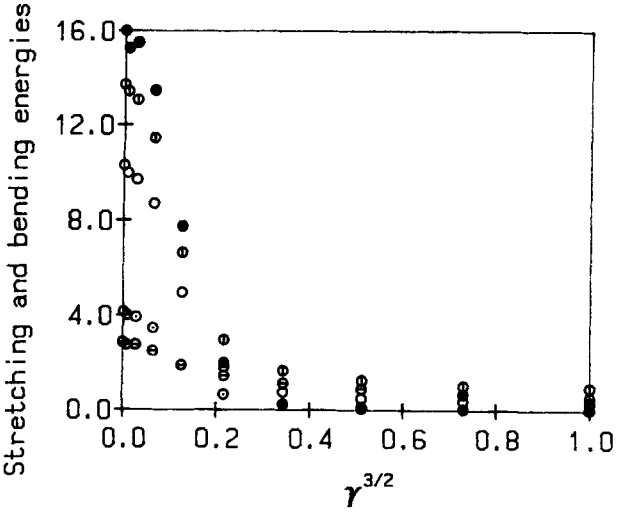

Figure 18 C—C bond stretching energy (⊙), C—H bond stretching energy (●), C—C—C bond angle bending energy (⊖), C—C—H bond angle bending energy (◫), and H—C—H bond angle bending energy (○) of model III for *i*-butane.

4 CONCLUSION

In this paper, we have presented NEMD simulations of three different models for *n*-butane and *i*-butane. We found that all the strain dependent viscosities of model I, II, and III for *n*-butane and *i*-butane exhibited a shear-thinning and a linear dependence

on $\gamma^{1/2}$, and that the viscosity of *i*-butane is predicted by model I and II to be less than that of *n*-butane (branching lowers the viscosity). However for model III which is an atomistically detailed model, the calculated viscosity of *i*-butane is higher than that of *n*-butane (branching increases the viscosity) as observed experimentally, even though it does not yield quantitative agreement with the viscosity of either the *n*-butane or *i*-butane. This suggests that the inclusion of H atoms may be important in correctly predicting the effect of molecular structure on alkane rheology.

Acknowledgements

The authors thank to Pittsburgh Supercomputer Center for the access to the Cray-YMP and to Korea Institute of Science Technology for the access to the Cray-c90 system. One of the authors (P. T. C.) gratefully acknowledges the support of this research by the National Science Foundation through grant CTS-910136. S. H. L. gratefully acknowledges the support of this research by the Korea Research Foundation through Non-Directed Research Fund, 1994.

References

[1] P. T. Cummings and D. J. Evans, "Nonequilibrium molecular dynamics approaches to transport propertiees and non-Newtonian fluid rheology", *Ind. Eng. Chem. Res.*, **31**, 1237 (1992).
[2] R. Edberg, G. P. Morriss and D. J. Evans, "Rheology of n-alkanes by nonequilibrium molecular dynamics", *J. Chem. Phys.*, **86**, 4555 (1987).
[3] G. P. Morriss, P. J. Daivis and D. J. Evans "The rheology of *n*-alkanes: Decane and eicosane", *J. Chem. Phys.*, **94**, 7420 (1991).
[4] P. J. Daivis, D. J. Evans and G. P. Morriss, "Computer simulation study of the comparative rheology of branched and linear alkanes". *J. Chem. Phys.*, **97**, 616 (1992).
[5] P. J. Daivis and D. J. Evans, "Comparison of constant pressure and constant volume nonequilibrium simulations of sheared model decane". *J. Chem. Phys.*, **100**, 541 (1994).
[6] J. P. Ryckaert and A. Bellemans, "Molecular dynamics of liquid alkanes". *Discuss. Faraday Sco.*, **66**, 95 (1978).
[7] R. Edberg, D. J. Evans and G. P. Morriss, "Constrained molecular dynomics: Simulations of liquid alkanes with a new algorithm", *J. Chem. Phys.*, **84**, 6933 (1986).
[8] P. A. Wiolopolski and E. R. Smith, "Dihedral angle distribution in liquid n-butane: Molecular dynamics simulation", *J. Chem. Phys.*, **84**, 6940 (1986).
[9] A. Baranyai and D. J. Evans. "New algorithm for constrained molecular dynamics simulation of liquid benzene and naphthalene", *Mol. Phys.*, **70**, 53 (1990).
[10] H. C. Andersen, D. Chandler and J. D. Weeks, "Roles of repulsive and attractive forces in liquids: The optimized random phase approximation", *J. Chem. Phys.*, **56**, 3812 (1972).
[11] H. C. Andersen, D. Chandler and J. D. Weeks, "Roles of the repulsive and attractive forces in liquds. The equilibrium theory of classical fluids", *Adv. Chem. Phys.*, **34**, 105 (1976).
[12] S. Chynoweth, U. C. Klomp and L. E. Scales, "Simulation of organic liquids using pseudo-pairwise interatomic forces on a toroidal transputer array", *Comput. Phys.* Commun., **62**, 297 (1991).
[13] S. Chynoweth, U. C. Klomp and Y. Michopoulos, "Comment on: Rheology of n-alkanes by non-equilibrium molecular dynamics", *J. Chem. Phys.*, **95**, 3024 (1991).
[14] A. Berker, S. Chynoweth, U. C. Klomp and Y. Michopoulos, "Non-equilibrium molecular dynamics (NEMD) simulations and the rheology properties of liquid *n*-hexadecane", *J. Chem. Soc. Faraday Trans.*, **88**, 1719 (1992).
[15] F. Muller-Plathe, "Diffusion of penetrants in amorphous polymers: A molecular dynamics study", *J. Chem. Phys.*, **94**, 3192 (1991).
[16] F. Muller-Plathe, "Molecular dynamics simulation of gas transport in amorphous polypropylene", *J. Chem. Phys.*, **96**, 3200 (1992).
[17] F. Muller-Plathe, S. C. Rogers and W. F. V. an Gunsteren, "Computational evidence for anomalous diffusion of small molecules in amorphous polymers", *Chem. Phys. Lett.*, **199**, 237 (1992).

[18] F. Muller-Plathe, S. C. Rogers and W. F. van Gunsteren, "Diffusion coefficients of penetrant gases in polyisobutylene can be calculated correctly by molecular dynamics simulations", *Macromolecules*, **25**, 6722 (1992).
[19] A. A. Gusev, F. Muller-Plathe, W. F. van Gunstrern and U. W. Suter, "Dynamics of small molecules in bulk polymers" in *Atomistic Modeling of Physical Properties*, edited by L. Monnerie and U. W. Suter (Springer-Verlag., Berlin, 1994).
[20] R. B. Bird, O. Hassager, R. C. Amstrong and C. F. Curtiss, *Dynamics of Polymeric Liquids Vol. 2: Kinetic Theory 2nd ed.* (Wiley, New York, 1977).
[21] J. W. Rudisill and P. T. Cummings, "The contribution of internal degrees of freedom to the non-Newtonian rheology of model polymer fluids", *Rheol. Acta.*, **30**, 33 (1991).
[22] J. W. Rudisill and P. T. Cummings, "Brownian dynamics siumulation of model polymer fluids in shear flow I. Dumbbell models", *J. Non-Newton. Fluid Mech.*, **41**, 275 (1992).
[23] J. W. Rudisill and P. T. Cummings, "Non-equilibrium molecular dynamics approach to the rheology of model polymer fluids", *Fluid Phase Eqil.*, **88**, 99 (1993).
[24] J. W. Rudisill, S. W. Fetsko and P. T. Cummings, "Brownian dynamics simulation of model polymer fluids in shear flow II. Bead-spring chain models" *Comput. Polymer Science*, **3**, 23 (1993).
[25] D. N. J. White and M. J. Boville, "Molecular mechanics calculations on alkanes and non-conjugated alkanes", *J. Chem. Soc. Perkin Trans.*, **2**, 1610 (1977).
[26] S. Toxvaerd, "Molecular dynamics calculation of the equation of state of alkanes" *J. Chem. Phys.*, **93**, 4290 (1990).
[27] F. Muller-Plathe, S. C. Rogers and W. F. van Gunsteren, "Gas sorption and transport in polyisobutylene: Equilibrium and nonequilibrium molecular dynamics simulations", *J. Chem. Phys.*, **98**, 9895 (1993).
[28] J. P. Ryckaert, I. R. McDonald and M. L. Klein, "Disorder in the pseudohexagonal rotator phase of n-alkane: molecular dynamics calculations for tricosane", *Mol. Phys.*, **67**, 957 (1989).
[29] D. J. Evans and G. P. Morriss, "Nonlinear response theory for steady planar Couette flow", *Phys. Rev.*, A **30**, 1528 (1984); ibid, "Non-Newtonian molecular dynamics" *Comput. Phys. Repts.*, **1**, 297 (1984).
[30] A. W. Lees and S. F. Edwards, "The computer study of transport processes under extreme conditions", *J. Phys. C: Solid State* **5**, 1921 (1972).
[31] T. Yamada and K. Kawasaki, "Application of mode-coupling theory to nonlinear stress tensor in fluids", *Prog. Theor. Phys.*, **53**, 111 (1975).
[32] K. Kawasaki and J. D. Gunton, "Theory of nonlinear transport processes: Nonlinear shear viscosity and normal stress effects" *Phys. Rev.*, A **8** 2048 (1973).
[33] M. H. Ernst, B. Cichocki, J. R. Dorfman, J. Sharma and H. J. van Beijeren, "Kinetic theory of nonlinear viscous flow in two and three dimensions", *J. Stat. Phys.*, **18**, 237 (1978).
[34] D. J. Evans, W. G. Hoover, B. H. Failor, B. Moran and A. J. C. Ladd, "Nonequilibrium molecular dynamics via Gauss's principle of least constraint", *Phys. Rev.*, A. **28**, 1016 (1983): A. D. Simmons and P. T. Cummings, "Non-equilinrium molecular dynamics simulation of dense fluid methane", *Chem. Phys. Lett.*, **129**, 92 (1986).
[35] M. P. Allen and D. J. Tildesley, *Computer Simulation of Liquids* (Oxford, Oxford Univ. Press., 1987).
[36] H. C. Andersen, "RATTLE: a velocity version of the SHAKE algorithm for molecular dynamics calculations", *J. Comp. Phys.*, **52**, 24 (1983).
[37] C. W. Gear, *Numerical Initial Value Problems in Ordinary Differential Equation* (Prentice-Hall, Englewood Cliffs, NJ, 1971).
[38] R. L. Rowley and J. F. Ely,"Non-equilibrium molecular dynamics simulations of structured molecules: Part I. Isomeric effects on the viscosity of butanes". *Mol. Phys.*, **72**, 831 (1991).
[39] G. Marechal and J. P. Ryckaert, "Atomic vs molecular description of transport properties in polyatomic fluids: *n*-butane as an example", *Chem. Phys. Lett.*, **101**, 548 (1983).
[40] K. Stephan and K. Lucas, *Viscosity of Dense Fluids* (Plenum, New York, 1979).
[41] S. H. Lee and P. T. Cummings, to be published.
[42] D. J. Evans, "Rheological properties of simple fluids by computer simulation", *Phys. Rev.*, A **23**, 1988 (1981).